

Integrative Approach for Polymorphic Crystallization Process Synthesis

Sze W. Lin, Ka M. Ng,* and Christianto Wibowo

Department of Chemical Engineering, Hong Kong University of Science and Technology, Clear Water Bay, Hong Kong, and ClearWaterBay Technology, Inc., 20311 Valley Boulevard, Suite C, Walnut, California 91789

This article presents an integrative approach for synthesizing a process to crystallize a specific polymorphic form. By considering crystallization compartments, metastable zones, and crystallization kinetics of different polymorphs, strategies for obtaining the desirable form can be developed. The progress of crystallization is followed by visualizing how the process paths move around different regions of a solid–liquid equilibrium phase diagram. Examples involving p-aminobenzoic acid, 2-(3-cyano-4-isobutyl-oxyphenyl)-4-methyl-5-thiazolecarboxylic acid, and two drug candidates are used to illustrate this approach.

Introduction

One of the most important issues in the development of crystallization processes for active pharmaceutical ingredients (APIs) is to obtain the desired polymorphic form of the product. While identical in chemical composition, polymorphs of the same API have different molecular arrangements in the crystal lattice, and exhibit markedly different physical and chemical properties. For example, their solubilities can be very different, affecting the bioavailability and efficacy of a drug. Polymorphs can have different shapes which in turn exert considerable influence on downstream processing steps such as filtration, washing, and bulk solids handling. Indeed, a polymorphic form is patentable. Thus, selecting the right polymorph for formulation and being able to produce it in a consistent manner are exceedingly important in pharmaceutical processing. However, finding all the polymorphs is difficult. Production can be challenging as well because interconversion among polymorphs may occur during and after the manufacturing process.^{1,2} A case in point is Ritonavir, an HIV drug discovered by Abbott Laboratories.³ When it was introduced in the market in 1998, many product lots of its semisolid capsule formulation failed the dissolution test. An investigation revealed a previously unknown, thermodynamically more stable, and less soluble crystalline form. This underscores the importance of the stability relationship between polymorphs.

Many specific polymorphic systems have been investigated in the literature, but only a few reports are available to rationalize process design by showing the relationships among the various polymorphs under different operating conditions. Davis and Desikan⁴ used a solvent composition versus temperature sketch to show regions where various polymorphic forms and liquid–liquid phase splits were found. This was then used to develop a strategy to obtain the desired polymorphic form of the pharmaceutical. Similarly, Spruijtenburg⁵ summarized all the experimentally obtained polymorphic forms under different crystallization temperatures and solvent compositions in a table format. Instead of sketches and tables, Wibowo et al.⁶ calculated and plotted solid–liquid equilibrium (SLE) phase diagrams with multiple solvents and polymorphs. The advantage of this representation is that the phase behavior can be properly and completely captured. In this study, an approach that combines the polymorphic SLE phase diagrams and crystallization kinetics is proposed for the synthesis of polymorphic crystallization processes.

Approach for Polymorphic Crystallization Process Design.

The approach consists of four steps/elements. The first step is to construct an SLE phase diagram, which provides the thermodynamic basis for crystallization-based separation synthesis. The second step is to determine crystallization kinetics such as nucleation and crystal growth rates. The third step is to determine metastable zone widths. Then, an operating strategy for recovering the desired form can be developed by tracing the process paths on the phase diagram. In practice, the sequence in which these steps are executed can vary. For example, crystallization kinetics can be determined before or after constructing the phase diagram. Also, the metastable zone width can be determined regardless of the availability of crystallization kinetics. Nevertheless, all four steps, irrespective of the order, need to be carried out in order to complete the synthesis task. This approach is expected to be iterative in nature, starting with a minimum amount of information and a simplified picture of the system, and gradually adding more details by revisiting all the steps.

Input Information

To initiate this approach, three types of information normally determined by the chemist are required: the number of polymorphs, characteristics of each polymorphic form, and stability relationship between polymorphs. The number of polymorphs is often obtained by experimental screening. In such an exercise, supersaturation is created by solventing-out, cooling, and/or evaporation to induce crystallization. The solids generated must be fully characterized. Details on the relevant analytical methods are available in the literature.⁷ High-throughput crystallization systems in which large arrays of conditions and compositions are processed in parallel can help reduce time and amount of material to complete the task.^{8–12}

Computational chemistry methods allow the prediction of possible crystal structures of a compound with known molecular structure.^{13–15} However, there is no guarantee that the predicted polymorph actually exists in nature. Also, no method can predict the exact number of polymorphs or the existence of hydrates and solvates, which may be more favorable for formulation and/or production.²

After identifying the polymorphs, the stability relationship between them should be determined next. For a pair of polymorphs, there are two types of stability relationship, namely monotropy and enantiotropy.¹⁶ If one polymorph is more stable than the other at any temperature, the polymorphs are monotropic to each other. However, if there is a transition temperature above and below which the stability order is reversed, the two polymorphs are enantiotropic. Various methods are available for the determination of transition temperature, ranging from

* Corresponding author. Fax: +852 2358-0054. E-mail: kekmng@ust.hk.

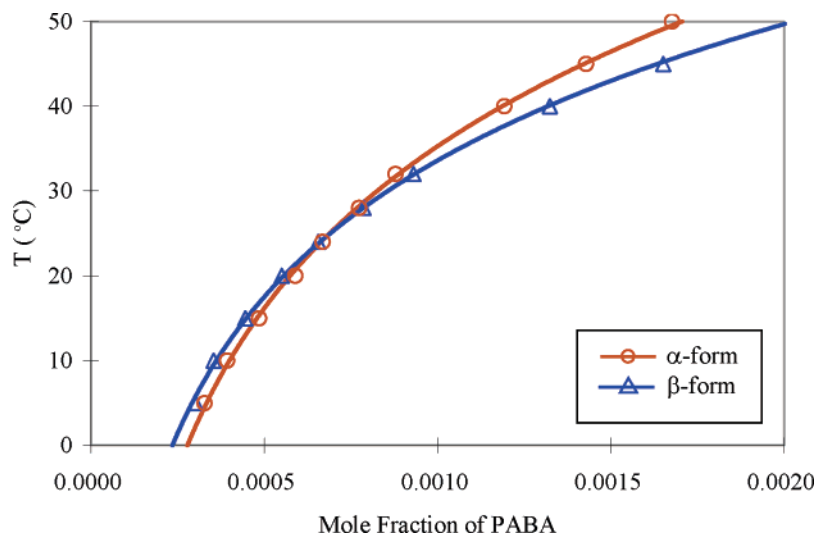


Figure 1. Phase diagram of PABA–water system.

computation^{17–19} to graphical solutions such as the van't Hoff plot^{20–22} and solubility diagram.^{23–25}

Each element of the integrative approach is now discussed below alongside an example related to the production of p-aminobenzoic acid (PABA)²⁶ in order to be more concrete. PABA has two polymorphic forms, α and β , which are enantiotropic with a transition temperature of 25 °C. Below this temperature, β is the stable polymorph. When water is used as a solvent for crystallization, no solvate is formed. For illustration purpose, both pure α form and pure β form are assumed to be the desired product. In addition, the crystallization process would operate below the transition temperature in order to use cooling water for crystallization.

Development of Phase Diagram. After selecting the solvents and antisolvents, if necessary, the equilibrium phase behaviors are represented in a phase diagram. Experimental determination of SLE phase diagrams has been discussed by Kwok et al.,²⁷ among others. The various types of SLE phase diagrams have been extensively discussed.^{28–32} The presence of solvates and compounds is of special relevance to pharmaceuticals.^{6,33,34} Lin et al.³⁵ demonstrated a procedure for capturing a chemist's recipe on SLE and LLE (liquid–liquid equilibrium) phase diagrams. LLE behavior may lead to oiling out during processing. For example, in drowning out crystallization, the solvent and antisolvent may be immiscible within a certain range of temperatures. If crystallization takes place in this immiscible region, liquid–liquid phase split causes the formation of droplets which may interfere with crystal growth. With a suitable phase diagram, strategies can be developed to keep the process path outside of this liquid–liquid immiscibility region.

PABA Example. Figure 1 shows a section of the phase diagram of the PABA–water system with temperature ranging from 0 to 50 °C. Solubility data are taken from the literature.²⁶

Determination of Crystallization Kinetics. In-line tools including Raman spectroscopy,³⁶ focused beam reflectance measurement (FBRM), attenuated total reflectance (ATR)-FTIR spectrometry,³⁷ and powder X-ray diffraction (PXRD) can be used for monitoring the crystallization process and thus the crystallization kinetics. These real time measurements can be replaced by periodic sampling,^{38,39} but the error in the kinetics data, obtained by regression, may be relatively large due to the time delay. Nonetheless, these experimentally determined kinetics data usually provide a good starting point for process synthesis.

PABA Example. Since kinetic data are not available in the literature, assumed kinetic parameters will be used in our analysis (Table 1).

Identification of Crystallization Compartments and Metastable Zones. In the absence of crystallization kinetics, the relative nucleation rates of the polymorphs can be used to guide process design. The Ostwald rule, which states that the least stable polymorph would be the first solid to be formed in crystallization, provides an initial guess. Although Ostwald's rule can be explained on the basis of irreversible thermodynamics, structural relationships, or a combined consideration of statistical thermodynamics and structural variation with temperature, it is not universally true.⁴⁰

To illustrate our approach, consider a sketch of a binary phase diagram (Figure 2a) where the two polymorphic forms of the solute exhibit enantiotropic phase behavior. Crystallization compartment for B is on the left, and that for A is on the right of the eutectic AB. Also shown are the metastable zones which can be experimentally determined.^{41–44}

In the system, A^I is the stable polymorph above the transition temperature while A^{II} is the stable polymorph below the transition temperature. If A^I is the target product, it is desirable to operate within region 1, which is entirely located above the saturation curve of A^{II} (unstable branch). This thermodynamically prohibits the crystallization of A^{II} and thus ensures the crystallization of A^I only. Note that, in the part of this region located within the A^I metastable zone, spontaneous nucleation of A^I may not occur. Seeding should be considered to induce the crystallization of A^I to shorten the processing time.

If the transition temperature is too high, the operation within region 1 is not desirable as it may lead to decomposition. In such a case, searching for a lower operating temperature region is necessary. Assuming that the Ostwald rule holds, region 2 is a good choice for the crystallization of A^I . Since both A^I and A^{II} are within their metastable zone limits in this region, the faster nucleation rate of A^I makes it crystallize first. To prevent solvent mediated transformation from happening, the crystallized A^I crystals should be promptly separated from the solvent.

On the other hand, if A^{II} is the desired product, region 3 is the ideal crystallization region. Similar to the case of region 1, this region is entirely located above the saturation curve of A^I and thus prohibits its crystallization. To ensure formation of A^{II} crystals within the A^{II} metastable zone, seeding may need to be used.

Table 1. Input Data for PABA Example

	Model Parameters	
liquid density (mol m ⁻³)	ρ	15000
solid α density (mol m ⁻³)	ρ_α	15000
solid β density (mol m ⁻³)	ρ_β	15000
volume shape factor	k_V	$\pi/6$
area shape factor	k_A	π
size of nuclei (m)	L_G^0	1×10^{-8}
α dissolution rate constant (m s ⁻¹)	$k_{D,\alpha}$	3.8×10^{-8}
β dissolution rate constant (m s ⁻¹)	$k_{D,\beta}$	1×10^{-7}
α growth rate constant (m s ⁻¹)	$k_{G,\alpha}$	9×10^{-6}
β growth rate constant (m s ⁻¹)	$k_{G,\beta}$	1×10^{-7}
α nucleation rate constant (no. s ⁻¹ m ⁻³)	$k_{n,\alpha}$	3×10^6
β nucleation rate constant (no. s ⁻¹ m ⁻³)	$k_{n,\beta}$	8×10^3
α and β nucleation exponent	n	1
α and β growth exponent	g	1
Solubility Curve (Fitted from Experimental Data)		
solubility of α	$x_\alpha^{\text{sat}} = 2.78 \times 10^{-4} \exp(3.63 \times 10^{-2} T)$	
solubility of β	$x_\beta^{\text{sat}} = 2.35 \times 10^{-4} \exp(4.31 \times 10^{-2} T)$	
Initial Fluid Composition		
amount of fluid in the crystallizer (mol)	m_{fluid}	100000
mole fraction of PABA	x_{PABA}	5.46×10^{-4}

Again assuming Ostwald's rule holds, region 4 is another choice for obtaining A^{II} crystals if the operating temperature in region 3 is too low, since it is within the metastable zone of

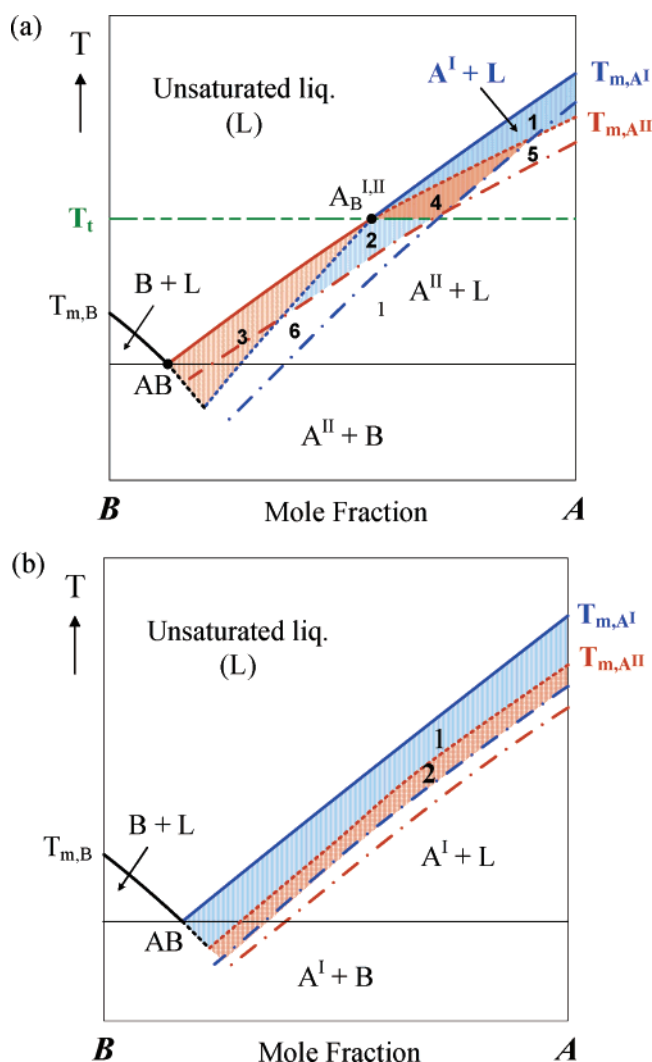


Figure 2. Isobaric SLE phase diagram showing different crystallization region for different forms: (a) enantiotropic system and (b) monotropic system.

the two polymorphs. In this region, A^{II} will first crystallize. As A^I is the stable polymorphic form in this region, the crystallized A^{II} solid should be promptly separated from the solvent to prevent solvent mediated transformation.

Operation in region 5, which is beyond the metastable limit of A^I but still within the metastable limit of A^{II}, or within region 6, which is beyond the metastable limit of A^{II} but within the metastable limit of A^I, leads to spontaneous nucleation of the stable form. If the unstable form crystallizes first according to the Ostwald rule, a mixture of stable and unstable forms would be initially obtained. However, if the processing time is sufficiently long, all the crystallized unstable form solids will transform to the stable form and thus only the stable polymorph is present at the end. Table 2 summarizes the conclusions of the above discussions.

Similar region identification can be performed for monotropic phase behavior. Figure 2b shows a binary phase diagram with polymorph A^I being the stable form and A^{II} the unstable form at all temperatures. If A^I is the target product, it is desirable to operate within region 1 as it is located above the saturation curve (unstable branch) of A^{II}. Region 2, which is a metastable zone shared by both A^I and A^{II}, is the ideal operating region for obtaining A^{II} if A^{II} has a higher nucleation and growth rates than A^I.

PABA Example. Since the PABA–water system exhibits enantiotropic behavior, the crystallization regions are similar to those shown in Figure 2a.

Development of Operating Strategies. A few heuristics are available to guide this activity (Table 3). In our approach, after constructing the phase diagram and subsequently identifying the metastable zones for crystallization, process paths based on known or assumed crystallization kinetics can be identified using mathematical models to find the best operating strategy. The liquid composition and product attributes such as particle size distribution are followed as a function of time. The potential of using techniques such as seeding to obtain the desirable polymorph can also be assessed. In this paper, we use the model developed by Schroer and Ng.⁵¹ In its simplest form, the mass balance equation for the liquid phase can be written as:

$$\text{accumulation} = \text{input} - \text{output} - \text{nucleation} - \text{growth} + \text{dissolution} \quad (1)$$

Table 2. Clarification of Metastable Zone in the Binary Enantiotropic System Shown in Figure 2a and the Corresponding Recommended Operation

region	location	desired product	recommended operations
1	within metastable zone of AI	AI	seeding with AI crystals
2	above saturation curve of AII	AI	shorter crystallization time
3	within metastable zone of AI and AII	AII	seeding with AII crystals
4	above saturation curve of AI	AII	shorter crystallization time
5	within metastable zone of AI and AII	AI	longer crystallization time
6	beyond metastable zone of AI	AII	longer crystallization time
	within metastable zone of AII		
	beyond metastable zone of AII		

Table 3. Design Heuristics for Polymorphic Crystallization

Seeding
consider using seeding if the desired polymorphic form is relatively unstable ^{37,45}
consider adding seeds in slurry form to facilitate growth, if the desired polymorphic form is neither the most stable nor unstable form ⁴⁵
seeding is not a feasible option if the solubility curve of the desired unstable form is below the metastable limit of a more stable form on the phase diagram ¹
Solvent-Mediated Transformation
consider crystallizing an undesired form first followed by solvent-mediated transformation to obtain the desirable form, if the existing solvent mainly lead to the crystallization of the undesired form ^{46,47}
consider using a different solvent, if the crystallization of the more stable form is the rate-limiting step in solvent mediated transformation ³⁹
consider using seed particles of smaller size or of different crystal habit, if the dissolution of the less stable form is the rate-limiting step in solvent mediated transformation ²⁵
Other Issues
consider using ultrasound for size reduction instead of milling or fast crystallization, if small particles are desired ⁴⁸
consider using additives such as the conformer or polymeric derivative of the desirable compound to inhibit the nucleation and/or growth of the undesired polymorphic forms ^{49,50}
for an enantiotropic system, do not operate a cooling crystallization process too close to the transition temperature, to prevent interconversion of the crystal modifications in the suspension ⁵

For example, if A is the desired polymorphic form, its liquid phase material balance can be written as follows:

$$\frac{dC_A V}{dt} = \rho_F x_A^F F - \rho_P x_A^P P - \rho_A k_V (L_{G,A}^0)^3 V B_{n,A}^0 - \rho_A A_A G_A / 2 + \rho_A A_A D_A / 2 \quad (2)$$

where the rates of nucleation (B^0) and growth (G) can be related to supersaturation (σ) via power law forms.

$$B_{n,A}^0 = k_{n,A} \sigma_A^n \quad (3)$$

$$G_A = k_{G,A} \sigma_A^g \quad (4)$$

The supersaturation, σ , is defined as:

$$\sigma_A = \frac{x_i - x_A^{\text{sat}}}{x_A^{\text{sat}}} \quad (5)$$

where x_i is the mole fraction of the crystallizing component in the liquid phase and x_A^{sat} is the corresponding composition at saturation. The dissolution term is only applicable when the polymorph is undersaturated. The rate law for dissolution is expressed as:

$$D_A = k_{D,A} \frac{x_A^{\text{sat}} - x_i}{x_A^{\text{sat}}} \quad (6)$$

The moment equations used to calculate the total area and mass of crystals formed are not repeated here. The numerical computation has been implemented using Matlab (Mathworks, Inc.).

Since the input information is unlikely to be reliable or complete, particularly at the beginning of a process synthesis project, it is critical that all predictions be compared with experimental results as far as possible. All four steps of the procedure should be repeated in an iterative manner when new physical and chemical properties, improved model parameters, crystallization experimental data, etc. become available.

PABA Example. As stated in the objective, two cases are considered: (1) recovery of pure α -form below the transition temperature and (2) recovery of pure β -form in the same temperature range. Assuming that the system obeys the Ostwald rule, the unstable α -form has a faster nucleation rate than that of the stable β -form. Therefore, to obtain pure α -form crystals, we should consider fast cooling crystallization followed by prompt separation of the crystals from the solvent to prevent solvent mediated transformation. Ideally, the process path should stay within the metastable region of β -form (region 2 in Figure 2a), so that spontaneous nucleation of the β -form is averted. Seeding can also be considered as suggested by the heuristics (Table 3).

In contrast, to recover β -form crystals, crystallization within the metastable region of β -form where the α -form is unsaturated (region 3 in Figure 2a) is desirable. Alternatively, we can operate within the supersaturation region of both forms (region 2 or 6 in Figure 2a) and rely on solvent mediated transformation to allow any crystallized α -form crystals to transform to β -form.

In any case, cooling rate plays a key role in determining the actual process path. With the kinetics in Table 1, the influence of cooling rate on polymorph formation can be studied by simulations. The cooling crystallization process starts at 20 °C and terminates at 5 °C. Figure 3 shows the process paths under different cooling rates on the phase diagram while Figure 4 shows the amount of polymorphs produced in each case. These results are consistent with the experimental findings reported by Gracin and Rasmuson.²⁶

The red curve in Figure 3 is the process path under an exceedingly slow cooling rate of 0.6 °C/h. Fast nucleation of the α -form initially leads to the crystallization of only this form, and the process path coincides with its solubility curve. However, due to their instability in this temperature range, all the crystallized α -form crystals dissolve before the temperature reaches 5 °C (Figure 4a). Their disappearance leads to the nucleation and growth of β -form crystals. Therefore, the process path gradually moves away from the α -form saturation curve, turns to the β -form saturation curve and ends at point 2a in Figure 3. The blue line represents the process path under a cooling rate of 5 °C/h. At this relatively fast cooling rate, the process path quickly passes through the saturation curve of the

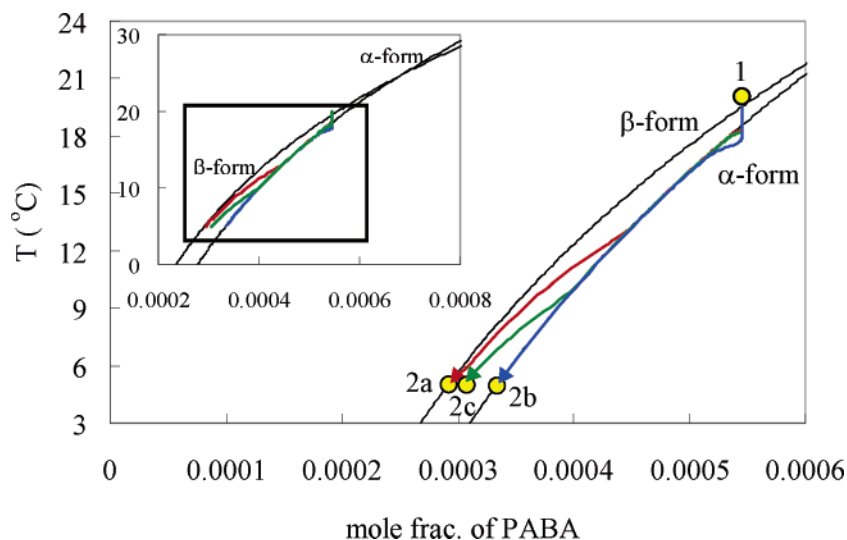


Figure 3. Phase diagram with process paths in the PABA example. The red, green, and blue lines represent the process paths under exceedingly slow (0.6 °C/h), moderate (1 °C/h), and relatively fast (5 °C/h) cooling rates, respectively.

unstable α -form to the region in which both forms are supersaturated. Since the α -form nucleates faster, it crystallizes first and provides seeds for subsequent growth. The fast cooling rate does not allow enough time for the stable β -form to nucleate, and the process path is close to the saturation curve of the α -form. By the time the temperature reaches 5 °C, no β -form has formed (Figure 4b) and the process path terminates on the saturation curve of α -form (point 2b, Figure 3).

When the cooling rate is in between at 1 °C/h, some unstable α -form crystals dissolve, leading to the nucleation and growth of the stable β -form crystals. When the crystallization terminates at 5 °C, not all the crystallized α -form crystals have dissolved and thus both α -form and β -form crystals are found at the end (Figure 4c). The green curve in Figure 3 represents the process path under such a cooling rate.

Additional Examples

Three more examples are discussed below to explore different facets of this approach:

Example 1. Purification Process of a Reaction Product. MK-A is a development compound at Merck.⁴⁶ It has four polymorphs, A, B, C, and E. MK-A form B is monotropic with respect to both forms A and C, and it is comparatively less stable. Forms A and C are enantiotropic, and the transition temperature is 21 °C. Above this temperature, A is the stable form. DSC data indicate that the melting points of A and C are 186 and 170 °C, respectively. Form E can be obtained by drying the solvate formed when MK-A is crystallized in *N*-methyl pyrrolidinone (NMP) as solvent. When water is used as a solvent, two hydrates, a hemihydrate (HH) and dihydrate (DH), are formed between MK-A and water. Below 31 °C, hemihydrate transforms to dihydrate and vice versa. Also, it is known that when the relative humidity is below 60%, dihydrate readily dehydrates to anhydrous polymorph A. Unlike water and NMP, isopropyl acetate does not form a solvate with MK-A. Some of these stability relationships among the various polymorphs and hydrates are summarized in Figure 5.

In the last synthesis step of MK-A, a mixture of form C and hemihydrate solids (semipure) is obtained. In this example, a strategy for synthesizing form A, the desired polymorphic form, from the semipure solid above the transition temperature (21 °C) will be developed. To increase the degree of freedom of the system, a solvent should be used. Isopropyl acetate is chosen

as it does not form solvate with MK-A and its azeotrope with water helps to facilitate solvent removal by distillation.

Phase Diagram. With all of this information, a ternary phase diagram with MK-A, water, and isopropyl acetate (IPA) can be sketched (Figure 6). A polythermal projection showing the various crystallization compartments including those of thermodynamically stable polymorphs is shown on the triangular base.

Kinetic Behavior. Very limited qualitative information on kinetics is available. It is known that the transformation from a mixture of hemihydrate and form C to pure form C is instantaneous in dry isopropyl acetate. Also, the transformation of form C to form A is relatively long and should take place at a temperature higher than 22 °C with an amount of water less than 0.6 wt % in isopropyl acetate. In the absence of quantitative data, the kinetic parameters and solubility data are assumed (Table 4). With these parameters, the amounts of forms C and A in the system, calculated using the model developed by Schroer and Ng,⁵¹ match the experimental results using Raman spectroscopy for such a C to A transformation at 35 °C.⁴⁶

Crystallization Compartments and Metastable Zones. The MK-A crystallization compartment (yellow region) is ideal for the recovery of form A from the solution.

Strategy Development. Starting with a wet cake of form C and hemihydrate at temperature T1 (point 1 in Figure 6), there are two possible ways to get into the MK-A crystallization compartment (yellow region). We can remove the water in the system and then add isopropyl acetate. Or we can add isopropyl acetate to the system before removing water.

In the first alternative, removing water by drying moves point 1 to point 2 in Figure 6. As the hemihydrate releases water to transform to form C, a mixture which is richer in form C is obtained. Transformation to form A is unlikely under such a dry condition. Then, isopropyl acetate is added to the system so that point 2 moves to point 3. The ratio of the added isopropyl acetate to the remaining water determines the location of point 3 which must stay within the MK-A crystallization compartment to prevent the formation of hydrates. At point 3, form C crystals suspended in solvent undergo solvent mediated transformation to form A. With crystals of form A present as seeds, cooling of this solution produces more form A, as represented by the movement from point 3 to point 4.

In the second alternative, the addition of isopropyl acetate to the semipure wet cake moves point 1 to point 2' in the

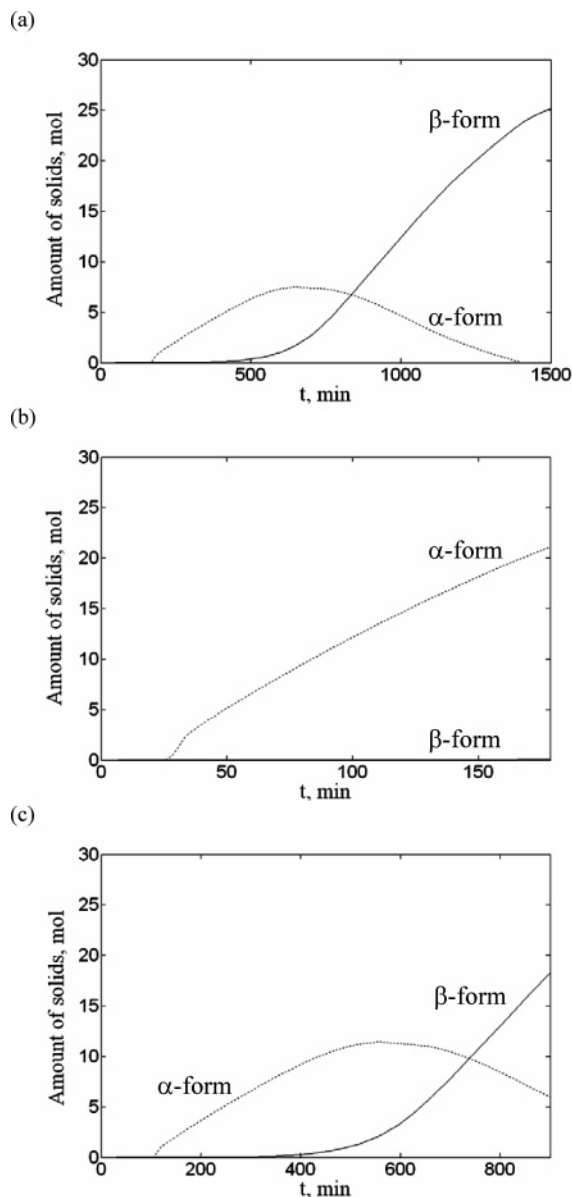


Figure 4. The amount of PABA polymorphs crystallized under different cooling rates: (a) 0.6 °C/h, (b) 5 °C/h, and (c) 1 °C/h.

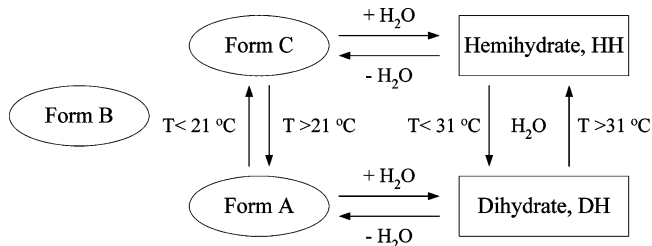


Figure 5. Stability relationship between polymorphs and hydrates in example 1.

unsaturated region (above the saturation surfaces). Then, removal of water by azeotropic distillation results in a composition such as point 3 in Figure 6. Since distillation occurs in the vapor–liquid equilibrium envelope, only the projection of the process path is drawn in Figure 6. Solvent mediated transformation and cooling then follow to produce pure form A.

With the crystallization kinetics in Table 4, solvent mediated transformation from form C to A at 35 °C is simulated by assuming that the initial concentration of MK-A in the solution is at the solubility limit of form C and the initial charge of form

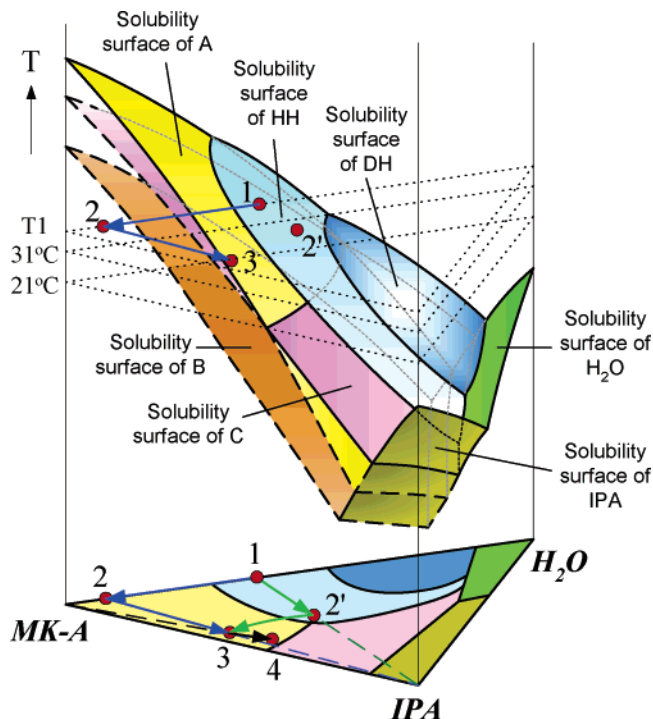


Figure 6. Polythermal phase diagram in example 1.

Table 4. Input Data for Solution Mediated Transformation Process in Example 1

Model Parameters at 35 °C		
liquid density (mol m ⁻³)	ρ	15000
solid C density (mol m ⁻³)	ρ_{SC}	15000
solid A density (mol m ⁻³)	ρ_{SA}	15000
volume shape factor	k_V	$\pi/6$
area shape factor	k_A	π
size of nuclei (m)	$L_{n,SA}^0$	1×10^{-8}
dissolution rate constant (m s ⁻¹)	$k_{D,SC}$	7.5×10^{-7}
growth rate constant (m s ⁻¹)	$k_{G,SA}$	1.125×10^{-6}
nucleation rate constant (no.s ⁻¹ m ⁻³)	$k_{n,SA}$	1×10^8
nucleation exponent	n	1
growth exponent	g	1
solubility of form C	x_C^{sat}	0.0279
solubility of form A	x_A^{sat}	0.0270
Initial Fluid Composition		
amount of fluid in the crystallizer (mol)	m_{fluid}	7
mole fraction of MK-A	x_S	0.0279
mole fraction of isopropyl acetate (IPA)	x_{IPA}	0.9721
Seed Characteristics		
amount of solid C (mol)	M_{SC}	0.7
particle size (m)	L_{SC}	1×10^{-4}
amount of solid A seed (mol)	M_{SA}	0
particle size (m)	L_{SA}	1×10^{-5}
Additional Model Parameters at 65 °C		
dissolution rate constant (m s ⁻¹)	$k_{D,SC}$	1.5×10^{-6}
growth rate constant (m s ⁻¹)	$k_{G,SA}$	2.25×10^{-6}
nucleation rate constant (no. s ⁻¹ m ⁻³)	$k_{n,SA}$	2×10^8
solubility of form C	x_C^{sat}	0.0743
solubility of form A	x_A^{sat}	0.0668

C solids is composed of particles of spherical shape and uniform size. Figure 7 shows the simulation results. It takes about 183 min for complete dissolution of form C (Figure 7a) during which nucleation and growth of form A occurs (Figure 7b). The supersaturation profile is shown in Figure 8. The relatively constant supersaturation during the initial 50 min indicates that the crystallization rate of form A balances the transformation rate. As the transformation nears completion, supersaturation is depleted toward the end of crystallization. Since the trans-

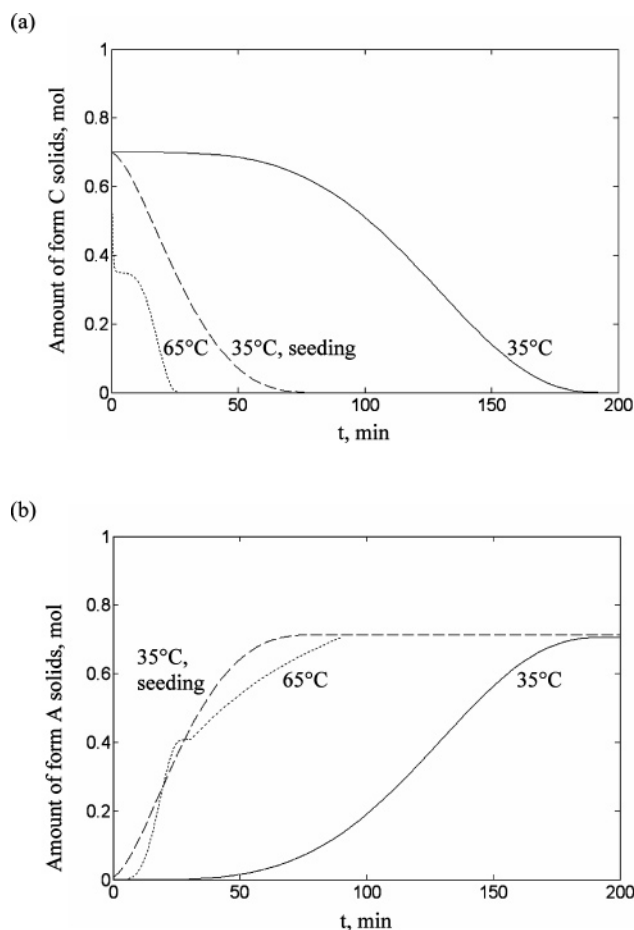


Figure 7. Number of moles of (a) form C and (b) form A solids versus time.

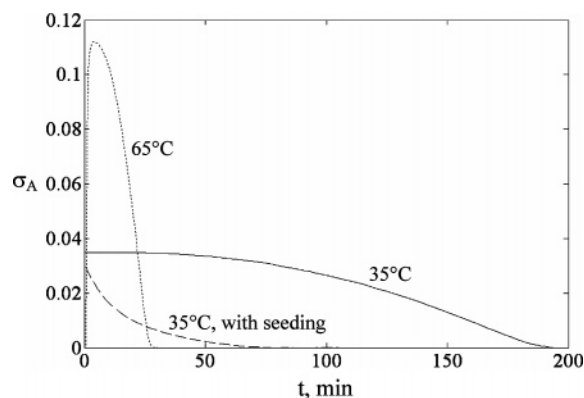


Figure 8. Supersaturation of form A versus time for different processes.

formation rate is quite slow, the feasibility of two potential improvements has been studied by modeling.

In the first improvement, the transformation temperature is increased from 35 to 65 °C. After the transformation is completed, cooling crystallization is performed by decreasing the temperature from 65 to 35 °C. The rationale behind this technique is that the solubility, dissolution, nucleation, and growth rate of forms C and A all increase with the temperature and so does the transformation rate. Once the transformation is finished, the crystallized form A solids can serve as seeds in cooling crystallization. Assuming that the crystallization kinetic constants at 65 °C double that at 35 °C (Table 4), the simulation results are shown as dotted curves in Figure 7.

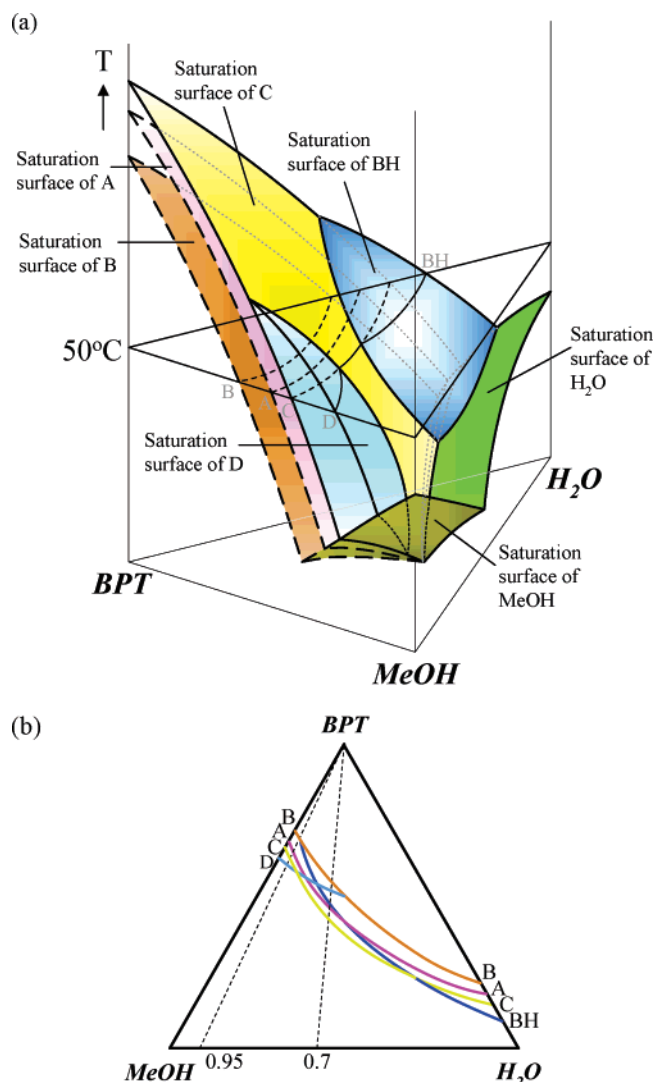


Figure 9. Phase diagram for example 2: (a) ternary polythermal phase diagram and (b) isothermal phase diagram at 50 °C.

When the starting temperature is changed from 35 to 65 °C, form C is now undersaturated for the same initial solution concentration. Therefore, it quickly dissolves and the concentration of MK-A in the solution increases until it exceeds the solubility of form A at 65 °C. The supersaturation of form A increases until the dissolution rate of form C is balanced by the nucleation and growth rate of form A. Afterward, further nucleation and growth of form A reduce the supersaturation until it is completely depleted (the dotted line in Figure 8). As shown in Figure 7a, the transformation is completed within 30 min. With enough seed crystals present, the system is cooled down to 35 °C at 0.5 °C per min. The same amount of product is formed as in the base case at 35 °C, but the processing time is shortened by half to about 90 min.

The second potential improvement is seeding with form A crystals at the beginning of the transformation process at 35 °C so as to promote crystal growth. In the simulation, the amount of form A seeds is 1% of the initial charge of form C solid. The seed particles are assumed to be of spherical shape and uniform size. As shown by the dashed curves in Figure 7a,b, the time for complete transformation is greatly reduced to 80 min, which is less than half of the time taken by the unseeded case. The supersaturation is depleted more rapidly than in the base case (Figure 8). Note that seeding at 35 °C is easier as no heating or cooling is involved.

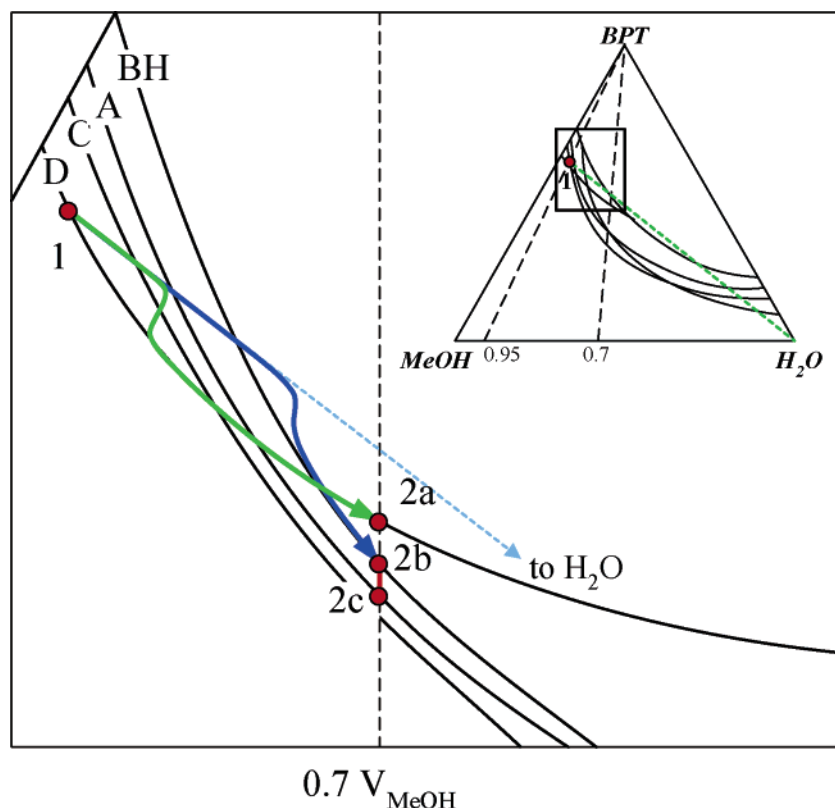


Figure 10. Process paths on the phase diagram in example 2.

All proposed alternatives should be experimentally verified. For example, we should perform the transformation and cooling process at 65 °C as well as the seeding experiment at 35 °C. To prevent hydrate precipitation during transformation, the boundary of the MK-A crystallization compartment should be located.

Example 2. Effect of Water Addition Rate on Polymorphic Crystallization. This example considers a system involving a thiazole derivative, 2-(3-cyano-4-isobutyl-oxyphenyl)-4-methyl-5-thiazolecarboxylic acid (BPT), which has three polymorphs, A, B, and C.⁵² A solvate D (BPT·MeOH) is formed with methanol, while another solvate BH (BPT·0.5H₂O) is formed with water. C is more stable than A at all temperatures and methanol compositions. In other words, A and C are monotropic to each other.

The objective of this example is to develop strategies to obtain pure form D, BH, and A (three separate cases) without much information on basic data such as heat of fusion and melting point of different polymorphic forms. The feed is BPT solution in methanol, and crystallization is effected by adding water as antisolvent.

Phase Diagram. Figure 9a shows a sketch of the phase diagram that is consistent with all the observations reported in the literature. B is suspected to be less stable than A, since limited information is available regarding this form and it always appears as BH during crystallization process. Therefore, the saturation surface of B is below that of A. On the other hand, the saturation surface of the more stable form C is above that of form A.

According to Kitamura and Nakamura,⁵² the thermodynamic stability of solvates BH and D is intensively influenced by the solution composition. At high methanol concentration, D is stable while BH is very unstable. On the other hand, if the methanol concentration is low, BH is more stable than D. Figure 9b shows

an isothermal cut at 50 °C to illustrate this stability relationship. The curves represent the solubility of different forms at 50 °C. At high methanol concentration, D is the most stable form followed by C, A, and BH. At low methanol concentration, BH is the most stable while D is the least stable.

Kinetic Behavior. Two pieces of qualitative information related to the rate of transformation between polymorphs are available in the literature. First, at a volume fraction of methanol in water (V_{MeOH}) of 0.95, crystals of A, BH, and C are very unstable and transform to D very quickly.⁵² Second, when V_{MeOH} is between 0.7 and 0.8, solvent mediated transformation from D, BH, and A crystals to the most stable C form crystals takes a long time.⁵³

Crystallization Compartments and Metastable Zones. Assuming that the system obeys Ostwald's rule at high methanol concentration, BH crystals appear first followed by forms A and C. Since the transformation rate of these polymorphs to form D is relatively fast and form D is the most stable form at high methanol concentration, this region is ideal for the crystallization of D.

At very low methanol concentration, BH can be recovered as the most stable form. However, since the transformation rate from different polymorphs to BH under these conditions is not known, there is no guarantee that this region is good for the crystallization of BH. As mentioned, the transformation rate to the most stable form C takes a long time at a moderate methanol concentration ($V_{\text{MeOH}} \approx 0.7$). As BH is rather unstable at such a concentration (compared to form A and C), this region may be the most suitable for the crystallization of BH provided that the crystals are promptly separated from the mother liquor.

According to the phase diagram, form A is the second most stable form at a moderate methanol concentration ($V_{\text{MeOH}} \approx 0.7$). Again, as the transformation rate to the stable form C is very slow, this region may be favorable for crystallizing form

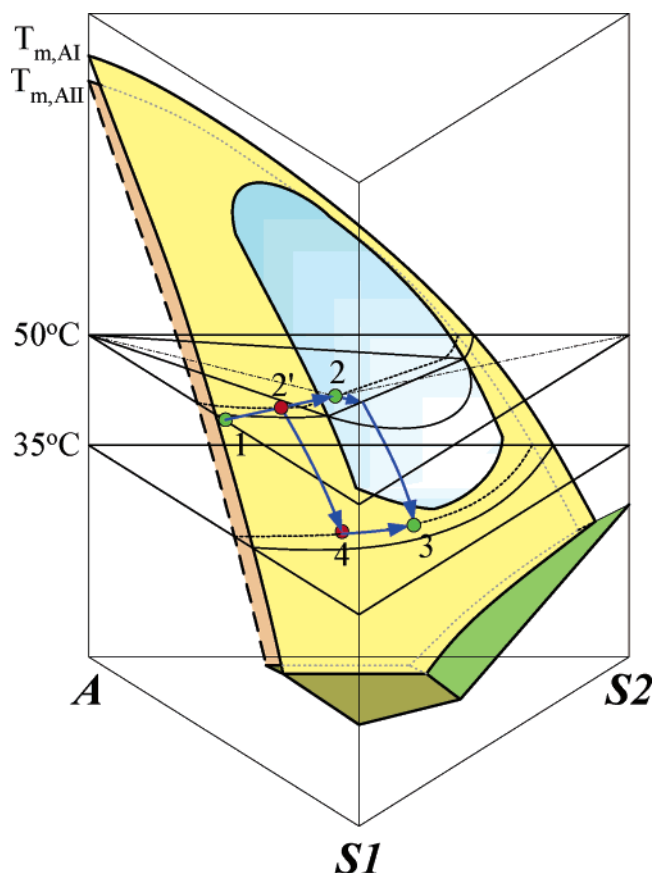


Figure 11. Isobaric ternary phase diagram in example 3. The system exhibits polymorphic phase behavior and liquid–liquid phase split. The solubility surface of polymorph AI is outlined by the solid line while AII is indicated by the dotted line.

A if it has a fast nucleation rate or the transformation from unstable forms (BH and D) to A is sufficiently fast.

Strategy Development. Strategies to recover D, BH, and A are then developed on the basis of the defined ideal crystallization region. To obtain form D crystals, crystallization must be done at a high methanol concentration environment. With a feed at point 1 ($V_{\text{MeOH}} = 0.95$), water is slowly added to the system to induce crystallization while the overall composition is still in the high methanol concentration region (Figure 10). In this way, crystallized unstable forms such as C would have enough time to transform into D. When methanol concentration decreases to a level where form D is no longer the most stable form, crystallization of form D continues since there is enough solid D in the system to serve as seeds to induce its own crystallization. Therefore, the process path (green curve in Figure 10) first ventures into the saturation region of C, leading to its crystallization. Transformation of C to D then brings the process path close to the saturation curve of D until the crystallization is completed at point 2a. The D crystals formed should be quickly filtered to prevent transformation to other forms.

The strategy to recover BH crystals is exactly the opposite. Fast water addition rate quickly brings the feed (point 1) to the moderate methanol concentration region where BH first crystallizes as it is the most unstable form. The process path (blue curve in Figure 10) approaches and follows the BH saturation curve until the crystallization endpoint (point 2b). Note that transformation of BH to D does not occur at such a moderate methanol concentration because D is now less stable than BH. To prevent transformation to A or C, the recovered BH crystals should be separated from the solution as soon as possible.

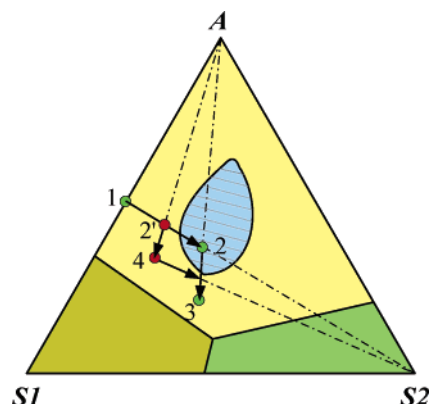


Figure 12. Polythermal projection of the phase diagram in example 3.

As moderate methanol concentration provides the ideal crystallization region for both BH and A crystals, the strategy for recovering form A is similar to that for recovering BH. However, the BH form obtained after the fast water addition process should be kept suspended in the solvent, such that it will undergo solvent mediated transformation to a more stable form. If the nucleation rate of form A is faster than form C, form A will crystallize first and the solution composition further moves from point 2b to point 2c on the saturation curve of A (Figure 10). Note that the time for such a transformation process should be carefully controlled in order to prevent further transformation from form A to C.

These developed strategies are consistent with the experimental observations described by Kitamura and Nakamura.⁵² Crystallization was carried out at 50 °C by adding water as an antisolvent to a mixture with a predetermined amount of BPT, water, and methanol. The volume fraction of methanol in water (V_{MeOH}) is decreased from 0.95 to 0.7, and the slurry formed was quickly filtered, dried, and then analyzed by XRD. It was observed that a slow water addition rate leads to formation of D while a fast water addition rate leads to formation of BH. Furthermore, the crystallized BH crystals left in solution would transform to A with time. It was found that the BH crystals completely transformed to form A crystals after 230 min. This is a strong indication that the nucleation rate of form A was relatively fast compared to that of form C, and the proposed strategy had worked well.

Example 3. Prevention of Oiling Out. The aim of this example is to illustrate the importance of visualizing the entire composition space in polymorphic crystallization process design. The drowning-out crystallization process of a drug candidate is considered.⁴⁸ Compound A has two polymorphs (AI and AII) exhibiting monotropic polymorphic phase behavior, with AI being the stable form. To recover A from its solution in solvent S1, an antisolvent S2 is added to induce crystallization. The objective is to recover crystals of the desired polymorphic form AII.

Phase Diagram. On the basis of initial experimental observations, crystallization of compound A in solvent S1 at 50 °C by adding antisolvent S2 leads to oiling out.⁴⁸ However, if the drowning-out crystallization process takes place at 35 °C, no oiling out is observed. This indicates that there is a liquid–liquid immiscibility region, which interferes with the solid–liquid region at 50 °C. On the other hand, no liquid–liquid immiscibility region exists at 35 °C. Figure 11 shows the sketch of an SLE phase diagram that is consistent with these observations. The yellow and orange surface represents the saturation surface of forms AI and AII, respectively. The blue surface represents the boundary of the liquid–liquid immiscibility region

in the system. The immiscibility region has a lower consolute temperature, which is slightly above 35 °C.

Kinetic Behavior. AII has a faster nucleation rate than that of AI, and the transformation from AII to AI is on the order of several hours.⁴⁸ Therefore, it is expected that AII crystals can be easily obtained once the solution becomes supersaturated.

Crystallization Compartments and Metastable Zones. Figure 12 is the polythermal projection of the phase diagram, showing the liquid–liquid immiscibility region and the saturation surfaces. The yellow area is the ideal crystallization compartment for A outside of the liquid–liquid phase split region. Operation within the blue region is not desirable because the presence of an oil suspension may inhibit crystal growth and affect product quality, especially when the process is scaled up.

Strategy Development. Strategies to recover AII crystals are developed at this stage. At 50 °C, S2 is added to the feed (point 1 in Figure 12). If S2 is added until the mixture reaches a composition represented by point 2, crystallization occurs together with liquid–liquid phase split. By cooling, more crystals are formed and the solution composition moves to point 3. As AII has a faster nucleation rate than AI, it will crystallize out first. The nucleation and growth of AII crystals can be promoted with the addition of AII seeds. To prevent solvent mediated transformation, crystallized AII solids should be promptly separated from the solvent. As observed by Kim et al.,⁴⁸ although this strategy does produce AII crystals, the resulting crystals are highly inhomogeneous due to the inclusion of oil droplets.

To prevent oiling out, the liquid–liquid region should be completely avoided. A smaller amount of S2 is added to the feed to produce point 2' (Figure 12), which is outside the liquid immiscibility region. As point 2' is still located within the compartment of A, cooling crystallization aided by seeding produces AII crystals, and the solution composition moves to point 4. More S2 is then added isothermally to induce crystallization of more AII crystals. The solution composition thus moves to point 3, which is the same end point as the previous alternative. As expected, Kim et al.⁴⁸ reported that this strategy produced good crystals.

Conclusions

Thermodynamics and kinetics are the controlling factors for polymorphic crystallization. An integrative approach, which combines fragmented and incomplete data, experimental observations, physical insights, and modeling related to these factors, has been developed for the development of a process to produce a desired polymorphic form. The approach begins with a representation of the equilibrium phase behavior of the system in the form of a phase diagram. The crystallization compartments and the metastable zones are identified. Crystallization kinetics is determined either qualitatively or quantitatively. The necessary experimental work, calculations, and polymorph recovery strategy development are expected to take place side-by-side in an iterative manner. This iterative scheme would converge to an optimum process that satisfies the overall objective.

The illustrative examples in this article focus on binary and ternary systems with two to three polymorphs to maintain clarity in visualization. However, this approach is applicable to higher dimensional systems with any number of polymorphs, provided that a convenient projection or cut is chosen for visualization. Systematic procedures for making projections and cuts are available.⁵⁴ For example, Davis and Desikan^{4,55} studied a system

involving four polymorphs, one solvate, and a liquid–liquid immiscibility phase. Such a problem can be handled using the same strategy.

The kinetic model used here utilizes the method of moments, which is capable of giving an overall picture of the crystallization process with minimum computational effort. However, without the particle size distribution, it cannot accurately describe complex phenomena such as size-dependent growth and dissolution rates. Therefore, a more rigorous model is desirable. Also, as the Ostwald rule may not hold and model parameters may not be readily available, it is crucial to develop systematic experimental methods to measure these parameters reliably and expeditiously. In particular, techniques for measuring the metastable zone of a particular polymorph at a given solution composition should be rationalized. Efforts in these directions are now underway.

Acknowledgment

We thank Joseph Schroer of ClearWaterBay Technology, Inc., for providing the computer code for kinetic calculations. Research support of the Research Grants Council (Grant HKUST602704) is gratefully acknowledged.

Nomenclature

- A_k = total area of crystals of component k , m²
- $B_{G,k}^0$ = nucleation rate for component k , no./s m³
- C_i = concentration of component i , mol/m³
- D = solid dissolution rate, m/s
- F = feed flow rate, m³/s
- g = crystal growth exponent, dimensionless
- G = crystal growth rate, m/s
- $\Delta H_{f,i}$ = heat of fusion of component i , J/mol
- k_A = area shape factor, dimensionless
- $k_{D,k}$ = rate constant for dissolution of component k , m/s
- $k_{G,k}$ = rate constant for crystal growth of component k , m/s
- $k_{n,k}$ = nucleation rate constant for component k , no./s m³
- k_V = volume shape factor, dimensionless
- $L_{G,k}^0$ = critical size of nuclei for growth of component k , m
- L_k = total length of crystals of component k , m
- m_{fluid} = amount of fluid in the crystallizer, mol
- M_k = total amount of crystals of component k , mol
- n = nucleation exponent, dimensionless
- P = product flow rate, m³/s
- R = universal gas constant, 8.314 J/mol·K
- T = temperature, K
- T_m = melting point, K
- V = volume of fluid in crystallizer, m³
- v_1 = constant evaporation rate, mol/s
- x_i = mole fraction of component i , dimensionless
- x_i^F = mole fraction of component i in the feed, dimensionless
- x_i^P = mole fraction of component i in the product, dimensionless
- x_i^{sat} = solubility of component i (in mole fraction), dimensionless

Greek Letters and Symbols

- ρ = fluid density, mol/m³
- ρ_i = density of solid i , mol/m³
- γ_i = activity coefficient of component i , dimensionless

σ_k = supersaturation with respect to solubility of component k

Literature Cited

- (1) Beckmann, W.; Otto, W.; Budde, U. Crystallization of the Stable Polymorph of Hydroxytriendione: Seeding Process and Effects of Purity. *Org. Process Res. Dev.* **2001**, *5*, 387.
- (2) Vippagunta, S. R.; Brittain, H. G.; Grant, D. J. W. Crystalline Solids. *Adv. Drug Delivery Rev.* **2001**, *48*, 3.
- (3) Chemburkar, S. R.; Bauer, J.; Deming, K.; Spiwek, H.; Patel, K.; Morris, J.; Henry, R.; Spanton, S.; Dziki, W.; Porter, W.; Quick, J.; Bauer, P.; Donaubaue, J.; Narayanan, B. A.; Soldani, M.; Riley, D.; McFarland, K. Dealing with the Impact of Ritonavir Polymorphs on the Late Stages of Bulk Drug Process Development. *Org. Process Res. Dev.* **2000**, *4*, 413.
- (4) Davis, W. P.; Desikan, S. A New Polymorph! Evolution of a Form Control Crystallization For a New Pharmaceutical Compound Under Development. *AICHE National Meeting*; Indianapolis, 2002.
- (5) Spruijtenburg, R. Examples of the Selective Preparation of a Desired Crystal Modification by and Appropriate Choice of Operating Parameters. *Org. Process Res. Dev.* **2000**, *4*, 403.
- (6) Wibowo, C.; Samant, K. D.; Ng, K. M. High-dimensional Solid-Liquid Phase Diagrams Involving Compounds and Polymorphs. *AICHE J.* **2002**, *48*, 2179.
- (7) Yu, L.; Reutzel, S. M.; Stephenson, G. A. Physical Characterization of Polymorphic Drugs: An Integrated Characterization Strategy. *PSTT* **1998**, *1*, 118.
- (8) Peterson, M. L.; Morissette, S. L.; McNulty, C.; Goldsweig, A.; Shaw, P.; LeQuesne, M.; Monagle, J.; Encina, N.; Marchionna, J.; Johnson, A.; Gonzalez-Zugasti, J.; Lemmo, A. V.; Ellis, S. J.; Cima, M. J.; Almarsson, O. Iterative High-Throughput Polymorphism Studies on Acetaminophen and an Experimentally Derived Structure for Form III. *J. Am. Chem. Soc.* **2002**, *124*, 10958.
- (9) Almarsson, O.; Hickey, M. B.; Peterson, M. L.; Morissette, S. L.; Soukasene, S.; McNulty, C.; Tawa, M.; MacPhee, J. M.; Remenar, J. F. High-Throughput Surveys of Crystal Form Diversity of Highly Polymorphic Pharmaceutical Compounds. *Cryst. Growth Des.* **2003**, *3*, 927.
- (10) Remenar, J. F.; MacPhee, J. M.; Larson, B. K.; Tyagi, V. A.; Ho, J. H.; McIlroy, D. A.; Hickey, M. B.; Shaw, P. B.; Almarsson, O. Salt Selection and Simultaneous Polymorphism Assessment via High-Throughput Crystallization: The Case of Sertaline. *Org. Process Res. Dev.* **2003**, *7*, 990.
- (11) Morissette, S. L.; Almarsson, O.; Peterson, M. L.; Remenar, J. F.; Read, M. J.; Lemmo, A. V.; Ellis, S.; Cima, M. J.; Gardner, C. R. High-throughput Crystallization: Polymorphs, Salts, Co-crystals and Solvates of Pharmaceutical Solids. *Adv. Drug Delivery Rev.* **2004**, *56*, 275.
- (12) Carlson, E. D.; Cong, P.; Chandler, W. H.; Desrosiers, Jr. P. J.; Freitag, J. C.; Varni, J. F. Apparatuses and Methods for Creating and Testing Pre-formulations and Systems for Same. U.S. Patent 6,939,515, 2005.
- (13) Leusen, F. J. J. Ab Initio Prediction of Polymorphs. *J. Cryst. Growth.* **1996**, *166*, 900.
- (14) Sacchetti, M.; Varlashkin, P. G.; Long, S. T.; Lancaster, R. W. Crystal Structure Prediction for Eniluracil. *J. Pharm. Sci.* **2001**, *92*, 1049.
- (15) Price, S. L. The Computational Prediction of Pharmaceutical Crystal Structures and Polymorphism. *Adv. Drug Delivery Rev.* **2004**, *56*, 301.
- (16) Burger, A.; Ramberger, R. On the Polymorphism of Pharmaceuticals and Other Molecular Crystals. I: Theory of Thermodynamic Rules. *Mikrochim. Acta* **1979**, *2*, 259.
- (17) Yu, L. Inferring Thermodynamic Stability Relationship of Polymorphs from Melting Data. *J. Pharm. Sci.* **1995**, *84*, 966.
- (18) Gu, C. H.; Grant, D. J. W. Estimating the Relative Stability of Polymorphs and Hydrates from Heat of Solution and Solubility Data. *J. Pharm. Sci.* **2001**, *90*, 1277.
- (19) Urakami, K.; Shono, Y.; Higashi, A.; Umemoto, K.; Godo, M. Estimation of Transition Temperature of Pharmaceutical Polymorphs by Measuring Heat of Solution and Solubility. *Bull. Chem. Soc. Jpn.* **2002**, *75*, 1241.
- (20) Kanke, M.; Sekiguchi, K. Dissolution Behavior of Solid Drugs. II. Determination of the Transition Temperature of Sulfathiazole Polymorphs by Measuring the Initial Dissolution Rates. *Chem. Pharm. Bull.* **1973**, *21*, 878.
- (21) Lagas, M.; Lerk, C. F. The Polymorphism of Sulphathiazole. *Int. J. Pharm.* **1981**, *8*, 11.
- (22) Park, K.; Evans, J. M. B.; Myerson, A. S. Determination of Solubility of Polymorphs Using Differential Scanning Calorimetry. *Cryst. Growth Des.* **2003**, *3*, 991.
- (23) Nass, K. K. Process Implications of Polymorphism in Organic Compounds. *AICHE Symp. Ser.* **1991**, *87*, 72.
- (24) Henck, J. O.; Bernstein, J.; Ellern, A.; Boese, R. Disappearing and Reappearing Polymorphs. The Benzocaine: Picric Acid System. *J. Am. Chem. Soc.* **2001**, *123*, 1834.
- (25) Veesler, S.; Lafferrere, L.; Garcia, E.; Hoff, C. Phase Transitions in Supersaturated Drug Solution. *Org. Process Res. Dev.* **2003**, *7*, 983.
- (26) Gracin, S.; Rasmuson, A. C. Polymorphism and Crystallization of p-Aminobenzoic Acid. *Cryst. Growth Des.* **2004**, *4*, 1013.
- (27) Kwok, K. S.; Chan, H. C.; Chan, C. K.; Ng, K. M. Experimental Determination of Solid-Liquid Equilibrium Phase Diagrams for Crystallization-Based Process Synthesis. *Ind. Eng. Chem. Res.* **2005**, *44*, 3788.
- (28) Dye, S. R.; Ng, K. M. Bypassing Eutectics with Extractive Crystallization: Design Alternatives and Tradeoffs. *AICHE J.* **1995**, *41*, 1456.
- (29) Dye, S. R.; Ng, K. M. Fractional Crystallization: Design Alternatives and Tradeoffs. *AICHE J.* **1995**, *41*, 2427.
- (30) Berry, D. A.; Dye, S. R.; Ng, K. M. Synthesis of Drowning-Out Crystallization-Based Separations. *AICHE J.* **1997**, *43*, 91.
- (31) Samant, K. D.; Berry, D. A.; Ng, K. M. Representation of High-Dimensional, Molecular Solid-Liquid Phase Diagrams. *AICHE J.* **2000**, *46*, 2435.
- (32) Harjo, B.; Wibowo, C.; Ng, K. M. Visualization of High-Dimensional Liquid-Liquid Equilibrium Phase Diagrams. *Ind. Eng. Chem. Res.* **2004**, *43*, 3566.
- (33) Byrn, S. R. *Solid State Chemistry of Drugs*; Academic Press: New York, 1982.
- (34) Giron, D. Investigations of Polymorphism and Pseudo-polymorphism in Pharmaceuticals by Combined Thermoanalytical Techniques. *J. Therm. Anal. Calorim.* **2001**, *64*, 37.
- (35) Lin, S. W.; Wibowo, C.; Ng, K. M. A Visual Approach for Integrating Chemistry Research and Process Design: Separation Process with Crystallization Steps. *Ind. Eng. Chem. Res.* **2005**, *44*, 6233.
- (36) Wang, F.; Wachter, J. A.; Antosz, F. J.; Berglund, K. A. An Investigation of Solvent-Mediated Polymorphic Transformation of Progesterone Using in Situ Raman Spectroscopy. *Org. Process Res. Dev.* **2000**, *4*, 391.
- (37) Doki, N.; Seki, H.; Takano, K.; Asatani, H.; Yokota, M.; Kubota, N. Process Control of Seeded Batch Cooling Crystallization of the Metastable α -Form Glycine Using and In-Situ ATR-FTIR Spectrometer and an In-situ FBRM Particle Counter. *Cryst. Growth Des.* **2004**, *4*, 949.
- (38) Kitamura, M. Crystallization Behavior and Transformation Kinetics of L-Histidine Polymorphs. *J. Chem. Eng. Jpn.* **1993**, *26*, 303.
- (39) Gu, C. H.; Young, V. Jr.; Grant, D. J. W. Polymorph Screening: Influence of Solvents on the Rate of Solvent-Mediated Polymorphic Transformation. *J. Pharm. Sci.* **2001**, *90*, 1878.
- (40) Threlfall, T. Structural and Thermodynamic Explanations of Ostwald's Rule. *Org. Process Res. Dev.* **2003**, *7*, 1017.
- (41) Beckmann, W. Seeding the Desired Polymorph: Background, Possibilities, Limitations, and Case Studies. *Org. Process Res. Dev.* **2000**, *4*, 372.
- (42) Teychene, S.; Autret, J. M.; Biscans, B. Crystallization of Eflucimibe Drug in a Solvent Mixture: Effects of Process Conditions on Polymorphism. *Cryst. Growth Des.* **2004**, *4*, 971.
- (43) Barrett, P.; Glennon, B. Characterizing the Metastable Zone Width and Solubility Curve Using Lasentec FBRM and PVM. *Trans Inst. Chem. Eng.* **2002**, *80*, 799.
- (44) Parsons, A. R.; Black, S. N.; Colling, R. Automated Measurement of Metastable Zones for Pharmaceutical Compounds. *Trans Inst. Chem. Eng.* **2003**, *81*, 700.
- (45) Beckmann, W.; Nickisch, K.; Budde, U. Development of a Seeding Technique for the Crystallization of the Metastable A Modification of Abecarnil. *Org. Process Res. Dev.* **1998**, *2*, 298.
- (46) Starbuck, C.; Spartalis, A.; Wai, L.; Wang, J.; Fernandez, P.; Lindemann, C. M.; Zhou, G. X.; Ge, Z. Process Optimization of a Complex Pharmaceutical Polymorphic System via In Situ Raman Spectroscopy. *Cryst. Growth Des.* **2002**, *2*, 515.
- (47) Okamoto, M.; Hamano, M.; Ooshima, H. Active Utilization of Solvent-Mediated Transformation for Exclusive Production of Metastable Polymorph Crystals of AE1-923. *J. Chem. Eng. Jpn.* **2004**, *37*, 95.
- (48) Kim, S.; Wei, C.; Kiang, S. Crystallization Process Development of an Active Pharmaceutical Ingredient and Particle Engineering via the Use of Ultrasonics and Temperature Cycling. *Org. Process Res. Dev.* **2003**, *7*, 997.
- (49) Davey, R. J.; Blagden, N.; Potts, G. D.; Docherty, R. Polymorphism in Molecular Crystals: Stabilization of a Metastable Form by Conformational Mimicry. *J. Am. Chem. Soc.* **1997**, *119*, 1767.
- (50) Blagden, N.; Davey, R. J.; Rowe, R.; Roberts, R. Disappearing Polymorphs and the Role of Reaction By-products: The Case of Sulphathiazole. *Int. J. Pharm.* **1998**, *172*, 169.

(51) Schroer, J. W.; Ng, K. M. Process Paths of Kinetically Controlled Crystallization: Enantiomers and Polymorphs. *Ind. Eng. Chem. Res.* **2003**, *42*, 2230.

(52) Kitamura, M.; Nakamura, K. Dependence of Polymorphic Transformation on Anti-Solvent Composition and Crystallization Behavior of Thiazole-Derivative Pharmaceutical. *J. Chem. Eng. Jpn.* **2002**, *35*, 1116.

(53) Kitamura, M.; Nakamura, K. Effects of Solvent Composition and Temperature on Polymorphism and Crystallization Behavior of Thiazole-Derivative. *J. Cryst. Growth.* **2002**, *236*, 676.

(54) Wibowo, C.; Ng, K. M. Visualization of High Dimensional Systems via Geometric Modeling with Homogeneous Coordinates. *Ind. Eng. Chem. Res.* **2002**, *41*, 2213.

(55) Desikan, S.; Parsons, R. L., Jr.; Davis, W. P.; Ward, J. E.; Marshall, W. J.; Toma, P. H. Process Development Challenges to Accommodate a Late-Appearing Stable Polymorph: A Case Study on the Polymorphism and Crystallization of a Fast-Track Drug Development Compound. *Org. Process Res. Dev.* **2005**, *9*, 933.

Received for review August 4, 2006

Revised manuscript received October 17, 2006

Accepted October 25, 2006

IE061026N